ELSEVIER

19 October 1998

PHYSICS LETTERS A

Physics Letters A 247 (1998) 313–318

Effects of particle trapping and velocity slippage on beam–plasma interactions

Hae June Lee, Jae Koo Lee, Indeog Bae, Min Sup Hur

Department of Physics, Pohang University of Science and Technology, Pohang 790-784, South Korea

Received 5 January 1998; revised manuscript received 30 June 1998; accepted for publication 5 August 1998
Communicated by M. Porkolab

Abstract

Nonlinear oscillations in homogeneous beam–plasma interactions are studied with respect to the trapping of beam particles and the velocity difference between the beam and the excited wave. A parameter defined as the ratio of bounce to oscillation frequencies divided by velocity slippage, is shown to be a good measure for the chaos in the system. The chaotic oscillation with a large value of this parameter is associated with a sideband instability. © 1998 Elsevier Science B.V.

PACS: 52.35.–g; 52.35.Qz; 52.40.Mj
Keywords: Beam–plasma instability; Sideband instability; Particle trapping; Velocity slippage; Chaos; Hybrid simulation

The beam–plasma instability is a primary phenomenon in systems with beam and plasma interactions. The nonlinear evolutions of weak beam–plasma instabilities have been studied extensively during the last 30 years [1–6]. Recently, the experimental investigation of self-oscillation and chaos in beam-injected plasma systems has received much attention [7–14]. The experiments are performed in an unmagnetized plasma device consisting of an electron-emitting cathode (with filaments around it) at one end and a current-collecting anode at the other end. There are two different modes in this system, anode glow and temperature limited modes. The oscillation mechanism in the anode-glow mode was explained by Greiner et al. [7,8], but that in the temperature limited mode (TLM) is still not clear. In this mode, the real system is bounded, inhomogeneous, and affected by the collisions of electrons and ions with neutral gas. But the injected electrons are accelerated in the cathode sheath to gain a sufficiently high energy for ionizing neutral gas and finally building up a homogeneous and dense plasma in the bulk region [8]. The velocity distribution of electrons in the bulk region is of the bump-on-tail type and the interaction of beam and plasma is similar to that of the beam–plasma instability in a homogeneous system [15]. It has been observed by using the XPDP1 code [16] that the oscillation frequencies and the growth rates of the high frequency oscillations in the TLM are similar to those of the beam–plasma instability.

In order to investigate the fundamental phenomena of the beam and plasma interactions, we simulated the simplified cases of the weak beam and the cold plasma interactions in a homogeneous system with a periodic boundary condition. We are concerned with the oscillations after the nonlinear saturation of the excited wave. After the saturation of the beam–plasma instability, the system approaches a metastable state

PII S0375-9601(98)00633-1

which is similar to the BGK mode [17]. The stability of this mode has been intensively studied for the last thirty years, and one of the dominant instabilities is known as the sideband instability due to trapped particles [18,19].

Recently, it was proved that a common parameter defined as the ratio of the interaction length to the slippage length is suitable as a simplifying measure of self-oscillation and chaos in other beam–plasma interacting systems, such as the extended Pierce diode [20,21] and the free electron laser (FEL) [22,23]. This parameter includes particle trapping and velocity slippage effects.

In this study, the oscillations in the beam–plasma instability after the nonlinear saturation are investigated. The effects of particle trapping and velocity slippage between the beam and the wave, which are related to the sideband instability and chaotic oscillation, are studied. Moreover, it is proved that the common parameter defined in the extended Pierce diode [20,21] and FEL [22,23] systems is also a good measure of chaos for this system.

We consider the system of a cold electron beam with density n_b and velocity v_b flowing through a homogeneous cold plasma with density n_p for the weak beam case ($R \equiv n_b/n_p \ll 1$). In such a system, it is possible to employ a hybrid code which uses the particle-in-cell method for the beam component and linearized fluid equations for the plasma component [24].

The dielectric function of this system is

$$\epsilon(k,\omega) = 1 - \frac{\omega_p^2}{\omega^2} - \frac{\omega_{pb}^2}{(\omega - kv_b)^2} \equiv \epsilon_p(\omega) - \frac{\omega_{pb}^2}{(\omega - kv_b)^2}, \tag{1}$$

where ω_{pb} and ω_p are the plasma frequencies of the beam and the bulk plasma, respectively, and ϵ_p is the dielectric function of the bulk plasma. The dispersion relation $\epsilon(k,\omega) = 0$ can be written as

$$1 - \frac{1}{W^2} - \frac{R}{(W-K)^2} = 0, \tag{2}$$

with the normalized frequency $W \equiv \omega/\omega_p$ and the wave number $K \equiv kv_b/\omega_p$. k and ω are the wave number and the oscillation frequency of the excited wave, which are the solutions of the dispersion relation. The single-wave trapping theory of Drummond et al. [4] gives an estimation of the saturation level of the field energy relative to the initial kinetic energy of the beam as

$$\frac{\frac{1}{4}\epsilon_0 E^2}{\frac{1}{2}mn_b v_b^2} \simeq \frac{2\Delta v}{v_b} \equiv s, \tag{3}$$

where E is the electric field intensity, ϵ_0 is the permittivity of free space, m is the electron mass, $\Delta v \equiv v_b - v\phi$ is the velocity difference between beam and wave, and s is defined as the velocity slippage. If the mode spectrum is dense and continuous, the most unstable mode with maximum growth rate at $K \simeq 1$ is allowed to grow, and the saturation level is known as about $\sqrt{3}(R/2)^{1/3}/2$. However, if the system does not allow the excitation of the most unstable mode, but allows only a single $K \neq 1$ mode, the saturation level and the oscillation patterns are modified. It was shown that the highest saturation level corresponds not to the fastest growing linear mode, but to the off-peak mode in the linear growth rate curve [25].

In this study, we generate a single mode for various K and observe the oscillations of the electrostatic field energy of the mode after nonlinear saturation. With a periodic boundary condition, the wave number is determined by the system length L as $k = 2n\pi/L$ with an integer number n. The maximum value of n is determined by the number of grids. In order to excite a single mode, we determine the system length L as small as the lowest mode $2\pi/L = (0.7\text{–}1.1)\omega_p/v_b$. With this value, the next mode $4\pi/L$ is $(1.4\text{–}2.2)\omega_p/v_b$, where the growth rate of the beam–plasma instability is zero for the weak beam case. Hence, only the lowest mode can be excited. This method is used in Ref. [25].

Figs. 1a and 1b are the time evolutions of the electrostatic field energies for $K = 0.8$ and 1.1. The values are normalized by the initial kinetic energy of the beam. Different from other nonlinear systems, the oscillation with a large electric field intensity ($K = 1.1$) is more regular than that with a small value ($K = 0.8$). This means there are other factors driving the system to chaos in addition to the electric field of the wave. Figs. 1c and 1d are the return maps for $K = 0.8$ and $K = 1.1$. The maps are obtained from the time series in Figs. 1a and 1b, with a proper time-interval, $\tau \sim \omega^{-1}$. The $K = 1.1$ case shows a limit-cycle oscillation with a closed circle, but the points are broadly scattered for $K = 0.8$, which means a chaotic oscillation. The power

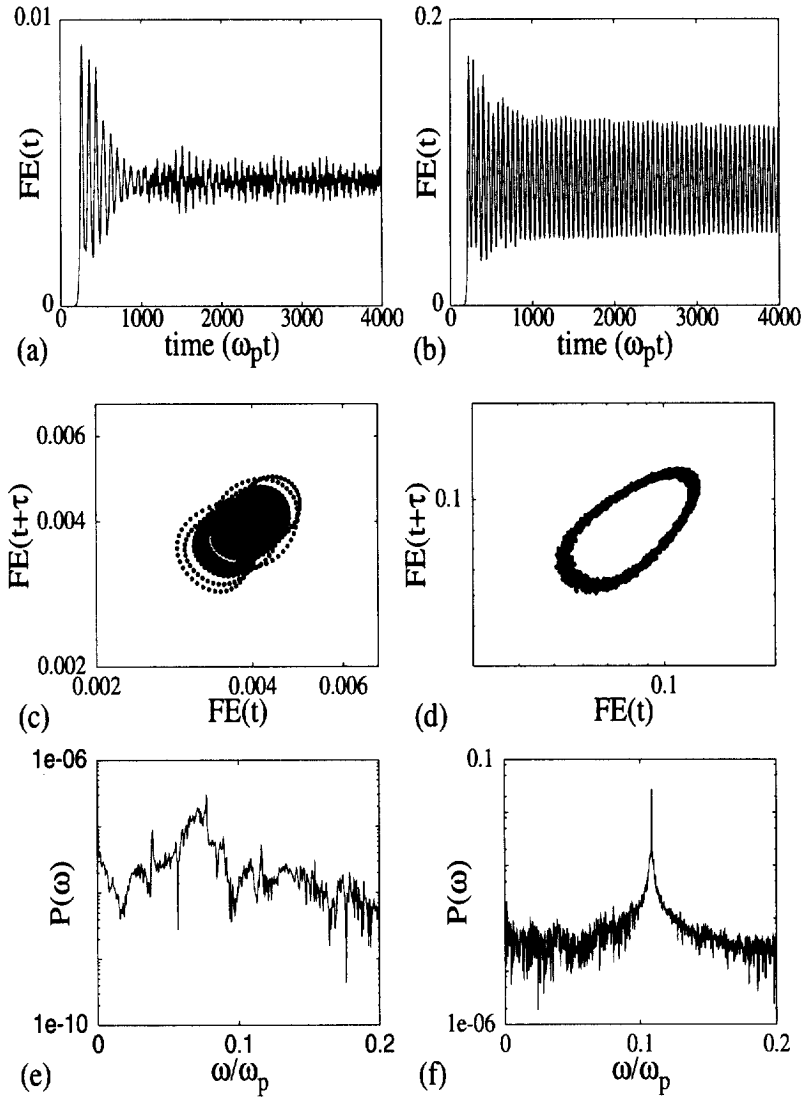

Fig. 1. The time evolutions of the electrostatic field energies for (a) $K \equiv kv_b/\omega_p = 0.8$ and (b) $K = 1.1$, return maps of the time series for (c) $K = 0.8$ and (d) $K = 1.1$, and the power spectra for (e) $K = 0.8$ and (f) $K = 1.1$.

spectra for these cases are shown in Figs. 1e and 1f. A broad spectrum is shown for $K = 0.8$, while there is a single peak for $K = 1.1$. The maximum peaks for each spectrum are the bounce frequencies of the oscillating trapped electrons. The simulation conditions are $R = 0.001$, $L/\Delta x = 2048$, $\Delta t = 0.05\omega_p^{-1}$, where L, Δx, and Δt are the system length, grid size, and time step, respectively. The number of simulated beam particles is 10^4.

These phenomena are explained by the sideband instability due to a trapped particle [18]. Kruer et al. [18] assumed that a large fraction of the beam particles are trapped in the trough of the wave due to its large amplitude, and those trapped particles move with a mean velocity equal to the phase velocity of the wave. Thus, these particles are able to act coherently like a beam. For simplicity, the particles are regarded to have a common frequency and to be grouped at the

bottom of the wave troughs. With these assumption, they derived a dispersion relation,

$$\epsilon(\tilde{k},\tilde{\omega}) = 1 - \frac{\omega_T^2}{(\tilde{\omega}-\tilde{k}v_\phi)^2-\omega_B^2} \times\left(\frac{1}{\epsilon_p(\tilde{k},\tilde{\omega})}+\frac{1}{\epsilon_p(\tilde{k}-2k,\tilde{\omega}-2\omega)}\right)=0, \quad (4)$$

where $\omega_B \equiv (ekE/m)^{1/2}$ is the bounce frequency, and $\omega_T = (n_T/n_b)^{1/2}\omega_{pb}$ is the plasma frequency of trapped particles with trapped-particle density n_T. ω_B is calculated with the maximum electric-field intensity after its saturation. The density ratio n_T/n_b, which is affected by the velocity slippage and amplitude of the wave, affects only the growth rate of the sideband mode. This ratio is about 0.8–0.9. k and ω are the solutions of Eq. (2). ϵ_p is the dielectric function of the background plasma, and $v_\phi = \omega/k$ is the phase velocity of the wave. The solution of Eq. (4) has growing modes. We define Δk and $\Delta\omega$ such that the growth rate $\tilde{\gamma}$ is maximum at $\tilde{k} = k \pm \Delta k$ (upper and lower sidebands), and $\Delta\omega = |\tilde{\omega} - \omega|$ at these values.

Fig. 2a shows the growth rates and oscillation frequencies of the sideband modes for $K = 0.8$ and $K = 1.1$. For $K = 0.8$, $\omega = 0.792\omega_p$, $\omega_B = 0.0767\omega_p$, the velocity slippage $s = 0.0212$, and the trapping ratio $n_T/n_b \simeq 0.83$ are found by the simulation. $\Delta\omega$ calculated by Eq. (4) is $0.195\omega_p$. For $K = 1.1$, $\omega = 0.982\omega_p$, $\omega_B = 0.108\omega_p$, $s = 0.215$, $n_T/n_b \simeq 0.85$, and the calculated $\Delta\omega$ is $0.0194\omega_p$. The maximum growth rate of the sideband as well as $\Delta\omega$ and Δk increase as K decreases. It is the reason for the chaotic oscillation for $K = 0.8$. In this figure, we can deduce the role of the velocity slippage in the sideband instability. In the theory, if ω_T, K, and ω are fixed, the growth rate and $\Delta\omega$ increase linearly with ω_B as shown in Fig. 2 of Ref. [18]. However, ω_T and ω as well as ω_B are changed for different K. In our results, the $K = 1.1$ case has a smaller growth rate and $\Delta\omega$, although it has larger ω_B than for $K = 0.8$. This is due to the velocity difference $v_b - v_\phi$ which increases as K increases. This factor affects the growth rate and $\Delta\omega$ of the sideband instability. Fig. 2b shows the dependences of $\Delta\omega$ and ω_B on K's. The difference in $\Delta\omega$ between simulation results and theory is due to the change of the plasma dielectric function ϵ_p by the contribution of trapped particles not included in Eq. (4). This factor increases the growth rate and frequency

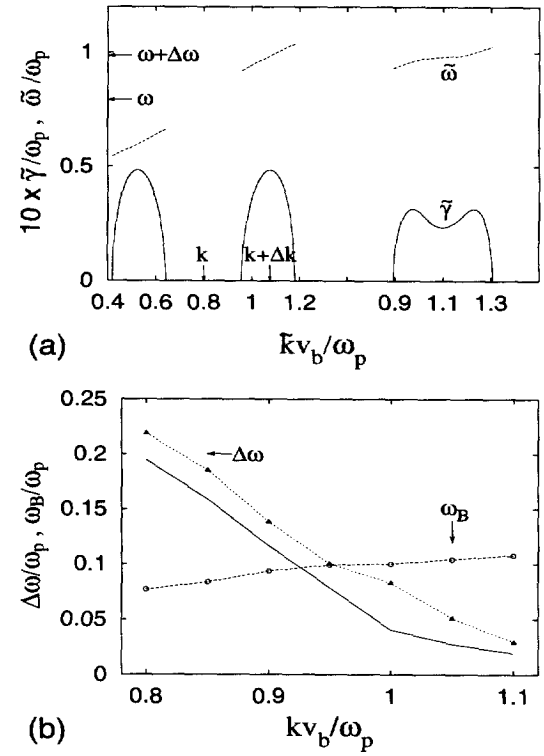

Fig. 2. (a) The growth rate $\tilde{\gamma}$ (solid lines) and real frequency $\tilde{\omega}$ (dashed lines) of the trapped-particle instability for $K = 0.8$ (left) and $K = 1.1$ (right). $\Delta\omega$ and Δk are obtained at the values of the maximum $\tilde{\gamma}$. The growth rates are magnified 10 times. (b) Simulated bounce frequencies (dashed line) and frequency-shift $\Delta\omega$ obtained from the theory (solid line) and the simulation (dotted line).

separation $\Delta\omega$ [19]. The effect of untrapped particles is also excluded in Eq. (4). $\Delta\omega$ becomes equal to ω_B around $K \simeq 0.95$, which is approximately the boundary between regular and chaotic oscillations.

The dominant factors driving the system to chaos are not only the large growth rate of sideband, but also the saturation level of it, which cannot be obtained from the linear theory. Fig. 3 shows the power spectra of the electrostatic potential at a given position (in the laboratory frame) for $K = 0.8$ and $K = 1.1$. Those are different from the spectra shown in Figs. 1e and 1f which are calculated with the field energy of the system. The power spectrum to the right side of the peak frequency ω_0 reflects the spectrum shown in Fig. 1e or 1f. The peak values in Figs. 1e and 1f are the bounce frequencies, which are shown in Fig. 3. The power spectra show also the amplitude of each side-

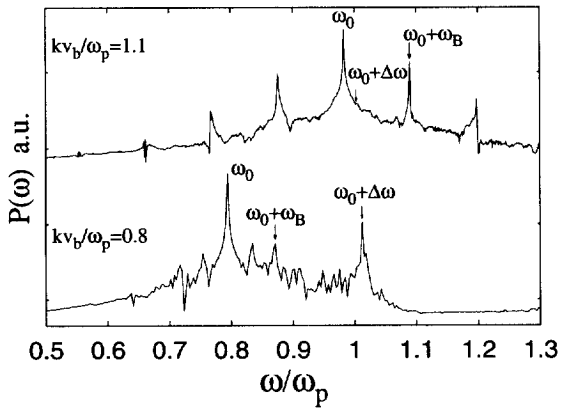

Fig. 3. Power spectra of the electrostatic potential at a given position for $K = 0.8$ (lower) and $K = 1.1$ (upper). ω_0 is the oscillation frequency of the excited wave. The sideband instability is dominant for $K = 0.8$.

band mode. Since the spectrum amplitude of $\omega_0 + \Delta\omega$ for $K = 0.8$ is comparable to that of $\omega_0 + \omega_B$, this mode is significantly affected by the sideband instability. Moreover, $\Delta\omega$ is larger than ω_B in this case. As a result, the oscillation is chaotic as shown in Fig. 1a. For $K = 1.1$, however, $\omega_B > \Delta\omega$ and the amplitude of sideband mode is much smaller than that of $\omega_0 + \omega_B$. This mode is hardly affected by the sideband and the regular oscillation is maintained for a long time as shown in Fig. 1b.

In FEL and Pierce diode systems, it was proved that a common parameter defined as the ratio of the interaction length to the slippage length is suitable as a simplified measure of the nonlinear and chaotic oscillation [20–23]. It includes the bounce frequency and the velocity slippage effects. The regimes where various oscillations such as single period (1P), two periods (2P), four periods (4P), and chaos (C) appear are indicated using this parameter. The parameter values (μ) exceeding approximately 2 are associated with the chaotic oscillations. The transitions of the FEL chaos [23] from 1P, to 2P, then to C occur at $\mu \sim 1.7$, and 2.0, which compare with the Pierce diode case [20] at $\mu \sim 1.8$, and 2.0. However, there is no period doubling route to chaos in the homogeneous beam–plasma system, since it is not a dissipative system. This deterministic parameter is almost independent of other input parameters. The equation of this parameter for the homogeneous beam–plasma system is

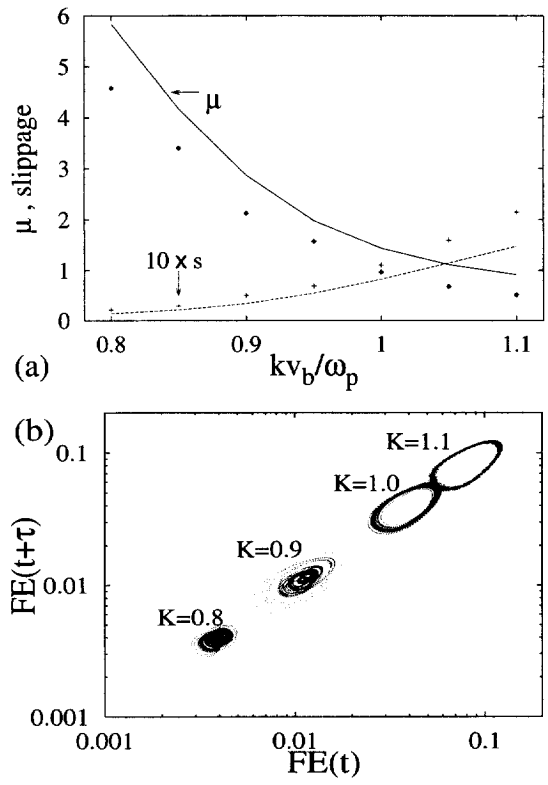

Fig. 4. (a) Deterministic parameter μ for the theory from Eq. (6) (solid line) with simulation results (dots) and velocity slippages ($s \equiv 2\Delta v/v_b$) for the theory (dashed line) with simulation results (plusses). The magnitudes of the slippage are magnified 10 times. (b) FE(t) versus FE($t+\tau$) return maps of field energies (FE) for various K, where $\tau = \omega^{-1}$ is the oscillation period of each mode.

$$\mu \equiv \frac{L_{\text{int}}}{L_{\text{syn}}} = \frac{\pi}{k}\left(\frac{2\pi v_\phi (v_b - v_\phi)}{\omega_B v_b}\right)^{-1} = \frac{\omega_B/\omega}{2(1 - v_\phi/v_b)}, \tag{5}$$

where $L_{\text{int}} (\equiv \pi/k)$ is the effective interaction length, and L_{syn} is the slippage length. The significance of the newly defined parameter μ is that the degree of the nonlinearity can be determined not only by the amplitude of the electric field but also by the difference between the beam and the wave velocities.

We derive this parameter with the linear approximation using Eq. (3) as

$$\mu(R, K, W) = \frac{\sqrt{K}}{W}\left(\frac{R}{4(1 - W/K)^3}\right)^{1/4}, \tag{6}$$

where W is obtained from the dispersion relation (2) for given K and R. The calculated values of the linear theory of Eq. (6) compared with the simulation results for various K are shown in Fig. 4a. As in the FEL and the Pierce diode systems, the oscillations are more stochastic for larger values of μ. μ is 4.5 for Fig. 1a, and 0.5 for Fig. 1b. This large μ for small K is due to the small slippage length which makes μ large despite the small ω_B. Fig. 4b shows the return maps of the time evolutions of the electrostatic field energies for $K = 0.8$, 0.9, 1.0, and 1.1. $K = 1.0$ and 1.1 show clear circles, which mean regular limit-cycle oscillations. As K decreases, this limit-cycle oscillation becomes stochastic. The boundary between these two oscillations is around $K \simeq 0.95$, where $\omega_B \simeq \Delta\omega$ as shown in Fig. 2b. The corresponding μ is $1.6\sim2$ by the simulation and the linear theory, Eq. (6). This value is similar to that of the FEL or Pierce diode, which is around 2.

In summary, we investigated the oscillations of electrostatic field energies of various single modes excited in the cold beam–plasma instability after nonlinear saturation using a hybrid code which employs the particle-in-cell method for the beam component and linearized fluid equations for the plasma component. For small kv_b/ω_p, the small velocity slippage makes the oscillation more chaotic despite the small saturation level. The mechanism of such a chaotic oscillation is associated with a sideband instability. It is clarified that a common parameter defined as the ratio of interaction length to slippage length is suitable as a diagnostic measure of the stochasticity in the beam–plasma system as shown in the FEL and the extended Pierce diode system. The larger this parameter is, the more chaotic the system, and the boundary between regular and chaotic oscillations is around 2.

The present studies were supported (in part) by the BSRI-Special Fund of POSTECH and the Basic Science Research Institute Program, Ministry of Education 1997, Project No. 97-2439.

References

[1] T.M. O'Neil, J.H. Winfrey, J.H. Malmberg, Phys. Fluids 14 (1971) 1204;
T.M. O'Neil, J.H. Winfrey, Phys. Fluids 15 (1972) 1514.
[2] S. Kainer, J. Dawson, R. Shanny, Phys. Fluids 15 (1972) 493.
[3] O. Ishihara, A. Hirose, A.B. Langdon, Phys. Rev. Lett. 44 (1980) 1404.
[4] W.E. Drummond, J.H. Malmberg, T.M. O'Neil, J.R. Thompson, Phys. Fluids 13 (1970) 2422.
[5] B. Goldstein, W. Carr, B. Rosen, M. Seidl, Phys. Fluids 21 (1978) 1569.
[6] N.G. Matsiborko, I.N. Onishchenko, V.D. Shapiro, V.I. Shevchenko, Plasma Phys. 14 (1972) 591.
[7] F. Greiner, T. Klinger, H. Klostermann, A. Piel, Phys. Rev. Lett. 70 (1993) 3071.
[8] F. Greiner, T. Klinger, A. Piel, Phys. Plasmas 2 (1995) 1810.
[9] T. Klinger, F. Greiner, A. Rohde, A. Piel, Phys. Plasmas 2 (1995) 1822.
[10] P.Y. Cheung, S. Donovan, A.Y. Wong, Phys. Rev. Lett. 61 (1988) 1360.
[11] J. Qin, L. Wang, D.P. Yuan, P. Gao, B.Z. Zhang, Phys. Rev. Lett. 63 (1989) 163.
[12] W.X. Ding, W. Huang, X.D. Wang, C.X. Yu, Phys. Rev. Lett. 70 (1993) 170.
[13] C.A. Capeau, G. Bachet, F. Doveil, Phys. Plasmas 2 (1995) 4650.
[14] C. Wilke, R.W. Leven, H. Deutsch, Phys. Lett. A 136 (1989) 114.
[15] H.J. Lee, J.K. Lee, Phys. Plasmas (1998), submitted.
[16] C.K. Birdsall, IEEE Trans. Plasma Sci. 19 (1991) 65.
[17] B. Bernstein, J.M. Greene, M.D. Kruskal, Phys. Rev. 108 (1957) 3.
[18] W.L. Kruer, J.M. Dawson, R.N. Sudan, Phys. Rev. Lett. 23 (1969) 838.
[19] M.V. Goldman, H.L. Berk, Phys. Fluids 14 (1971) 801.
[20] H.J. Lee, J.K. Lee, M.S. Hur, Y. Yang, Appl. Phys. Lett. 72 (1998) 1445.
[21] M.S. Hur, H.J. Lee, J.K. Lee, Phys. Rev. E (1998), to be published.
[22] S.J. Hahn, J.K. Lee, Phys. Rev. E 48 (1993) 2162; Phys. Lett. A 176 (1993) 339.
[23] S.J. Hahn, J.K. Lee, E.H. Park, T.H. Chung, Nucl. Instr. Meth. A 341 (1994) 200.
[24] J.K. Lee, C.K. Birdsall, Comput. Phys. Commun. 64 (1991) 214; Phys. Fluids 22 (1979) 1315.
[25] J.K. Lee, S.J. Hahn, IEEE Trans. Plasma Sci. 19 (1991) 52.